

Interpretation of Some Phenomena Observed in Southern California Stratus

J. G. EDINGER and M. G. WURTELE—*Department of Meteorology, University of California, Los Angeles, Calif.*

ABSTRACT—Extensive observations were made on aircraft flights in the marine layer over the Pacific Ocean off the coast of southern California. We interpret some of the cloud patterns as convective and some as gravity wave phenomena. The ship wave and the three-dimensional lee wave are observed and analyzed in terms of the accompany-

ing soundings, as are other characteristic cloud structures. From photographs of glories in the stratus tops, angles of back-scattering can be determined with sufficient accuracy to identify cloud-drop size distributions in accordance with Mie scattering theory.

1. INTRODUCTION

This study is an attempt to interpret, in terms of the appropriate theory, a variety of phenomena observed in a field investigation of the lower atmosphere off the coast of southern California during the summer of 1966 (Edinger and Wurtele 1969). The data were acquired from aircraft and of them we use chiefly visual observations from color photographs and soundings of temperature and humidity. The phenomena discussed are classifiable as convective, gravity wave, and optical.

First, however, because of the relative unavailability of the report by Edinger and Wurtele (1969), we give a brief account of the navigational and instrumental techniques employed in the field observations. A light aircraft, Cessna 136,¹ equipped with recording temperature, humidity, and altitude instruments, flew in the area from the coast out to a line connecting Santa Catalina, Santa Barbara, San Nicolas, and San Miguel Islands (fig. 1), sounding the lowest few thousand feet of the atmosphere every 15 or 20 mi of flight.

The temperature sensor used was a platinum-wire resistance element with a response time of about 0.01 s. A carbon-strip hygistor was used to determine relative humidity and a Meteorology Research, Inc. (MRI) recording altimeter provided the height above sea level. Determination of aircraft location was made by radio navigational aids, dead reckoning, and occasionally by radar tracking. A Moseley recorder provided continuous traces of temperature and humidity as a function of height. No instrumentation was carried for wind measurement, but qualitative information as to direction and speed could be deduced from observations of the state of the sea and from other visual observations.

Thirty-five flights were made from Aug. 1 to Sept. 28, 1966, during which over 800 individual "vertical" soundings of the atmosphere were recorded. Usually, the plane held a constant heading during the soundings;

although, in some special circumstances, spiral ascents and descents were made. Flights were confined to the daylight hours. Many pictures of the clouds and haze were taken to help in the interpretation of the data. Comments on the visible meteorological conditions were recorded by an observer.

2. STRATUS STRUCTURE

Perhaps the most frequent stratus pattern off the California coast is, simply, complete overcast with no discernible regular structure in the cloud deck. This has been interpreted by Neiburger (1944) as associated with an increase in the depth of the marine layer; that is, a lifting of the inversion layer by some mechanism that overcompensates the normal mean subsidence. This mean descending motion due to subsidence has been estimated to be quite small—less than 0.2 cm/s—in the area just west of the coast (Neiburger et al. 1961). The passage of even a minor synoptic trough may be associated with sufficient deepening of the marine layer to form a stratus deck. The most satisfactorily documented process is the diurnal oscillation of inversion height accompanying the horizontal expansion and contraction of the marine layer in the sea breeze (Neiburger 1944). At present, the stratus forecast techniques consist chiefly of attempts to predict inversion height as a function of the prognostic chart. A much-needed theoretical treatment has been begun by Lilly (1968), but there exists as yet no theoretical confirmation.

When a structured pattern is exhibited by the stratus, one of the most frequently observed is parallel rolls. These may be very uniform and regular in appearance, as in figure 2. This phenomenon must not be interpreted as billow clouds in the sense of gravity waves on the inversion surface. (See sec. 5.) In all cases of rolls observed in the present study, the wind direction was not perpendicular, but parallel, to the rolls. The explanation that suggests itself most readily in this case is convection under the

¹ Mention of a commercial product does not constitute an endorsement.

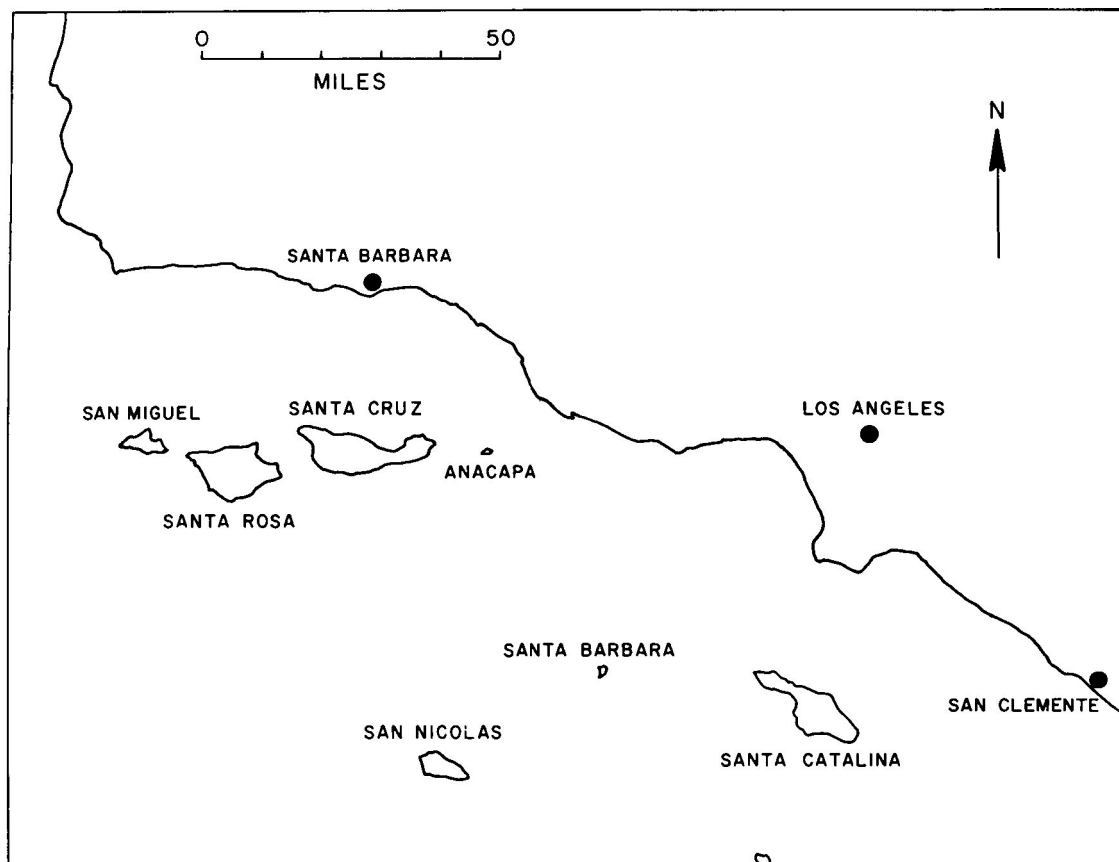


FIGURE 1.—Map of the Southern California coastal area.



FIGURE 2.—Longitudinal stratus rolls.

inversion. The appropriate theoretical model here is not that of Rayleigh, in which no mean flow exists, but that of Kuo (1963) extending the work of Eliassen et al. (1953). Their model is that of a statically unstable inviscid fluid with linear mean velocity profile. For small negative Richardson number, the horizontal scale of the rolls is several times the depth of the layer. This scale is consistent with that observed in figure 2, if one takes the depth of the marine layer as corresponding to the depth of the convective fluid.

The longitudinal convective roll must be associated with helical air-parcel trajectories in the marine layer. Such

trajectories have been observed in the lower atmosphere over Los Angeles from the motion of tracer balloons (Angell and Pack 1967).

If the layer is highly unstable statically and/or if there is a very light mean wind—both circumstances being exceptional over this region of the Pacific—the Richardson number will be large and negative. Then, according to the theory (Kuo 1963, pp. 210–211), the stabilizing effect of the shear is reduced, and the longitudinal rolls break up into a three-dimensional cellular structure. This is occasionally observed in the stratus, which can then resemble a huge system in Bénard convection. During the present

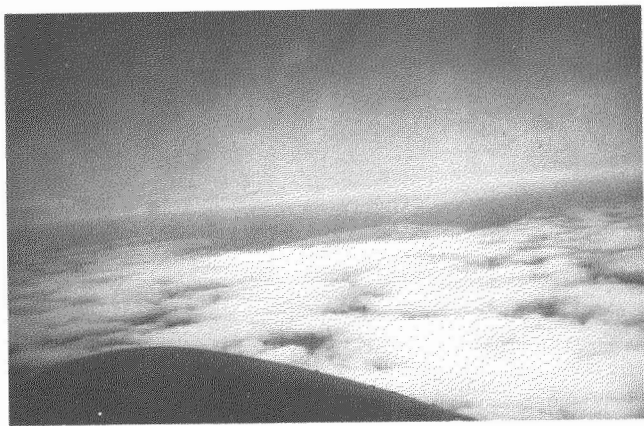


FIGURE 3.—Stratus in cellular patterns.



FIGURE 4.—Longitudinal rolls (right to left) and transverse gravity waves (bottom to top) in stratus. Flow is left to right, and San Nicolas Island is to the left.



FIGURE 5.—Gravity waves against the Santa Monica mountains. The coastline is to the right.

study, the best examples of this large negative Richardson number regime were those of figure 3. Here, again, the horizontal scale is two or three times the depth of the convecting fluid, consistent with the theory.

The occurrence of both rolls and cells has been recorded in the laboratory (Avsec 1939) and in nature (e.g., Malkus and Riehl 1954). The flights logged in the latter work were over the tropical Pacific (lat. 10° – 25°), and apparently cells were observed much more frequently than rolls (e.g., their fig. 3.36).

It may happen that some disturbance gives rise to gravity waves of various types that will be oriented normal to the wind direction. Figure 4 contains such an instance. The wind here is from left to right and there is an island off to the left under the clouds. The longitudinal roll pattern is clearly visible; but normal to the rolls, in the lee of the island, are wave crests of much greater amplitude. The distance between the crests is perhaps $1/4$ – $1/2$ mi so that, without confirming measurements, it would be difficult to interpret them as billow clouds. Another example of forced perturbations on the interface is contained in figure 5.

Here, the air is flowing right to left, just having come over the shoreline, and the wave crests are encountering

the Santa Monica mountains. The wavelength is about 1 mi, and again we hesitate to make a definite interpretation. These are the only two such examples we have, and our chief point is the infrequency or absence of the billow-cloud pattern that receives such emphasis in the textbooks.

There is, of course, a source of instability and presumably, therefore, of cloud bands, peculiar to the boundary layer (Faller 1965, Tatro and Mollo-Christensen 1967, Lilly 1966). This has become known as Ekman-layer instability and has two preferred modes depending on the Reynolds number. Following the nomenclature of Greenspan (1968), type B instability is the mode possibly most relevant to the cloud rolls of the marine layer. If a mean eddy transfer coefficient of about $15 \text{ m}^2/\text{s}$ is assumed, it follows from the experiments (Faller 1965, Tatro and Mollo-Christensen 1967, Lilly 1966) that a typical wavelength of about 4 km is predominant. This is consistent with our observations. However, the type B instability appears to derive from the characteristic curvature of the Ekman wind profile, and it is doubtful that the hypothetical conditions for this structure exist in the marine layer (Kao 1960). Observations are sadly lacking.

The secondary flow patterns computed by Brown (1970) are also a theoretically possible interpretation. There are,

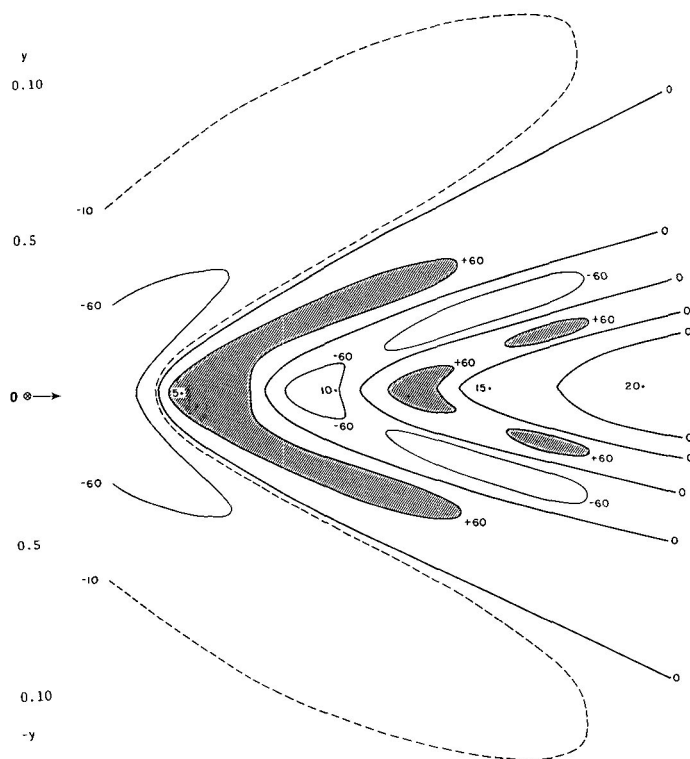


FIGURE 6.—Horizontal planform of vertical motion in the lee of an isolated mountain (after Wurtele 1957). The lines are equiscalar curves of vertical motion labeled in dimensionless units. Flow is left to right.

as yet, many uncertainties in this analysis, which is not confirmed by the turbulence computations of Deardorff (1970). On the whole, we prefer to hold to the hypothesis that the banded and cellular clouds of the marine layer are primarily convective in origin.

3. GRAVITY WAVES

When a fluid with continuously distributed stable stratification passes over an obstacle limited in the direction normal to the flow, an interesting three-dimensional internal gravity wave is produced. This has been computed theoretically by Wurtele (1957), who cites confirmation both in laboratory experiments and in nature (cf. Scorer 1956). The theoretically computed crescent-shaped areas of vertical motion, concave downwind, are reproduced in figure 6. The horizontal scale is that of the typical internal gravity wave, 5–10 km.

An example of this pattern is seen in the lee of San Nicolas Island (fig. 7). The wind is flowing right to left into a crescent-shaped pattern of descending motion. To use this as an example of the theoretical model mentioned above, we must know that the cloud in this case lies in a layer with continuous static stability, because the concentrated stability of an interface produced a very different pattern. The sounding of figure 8, taken at the time of the occurrence in figure 7, verifies this condition. The saturated marine layer is not neutrally stratified, as it usually is, but in this case is almost isothermal.



FIGURE 7.—Crescent-shaped downdraft area in the lee of San Nicolas Island. Flow is right to left, and the downwind edge of the island can be seen in lower right.

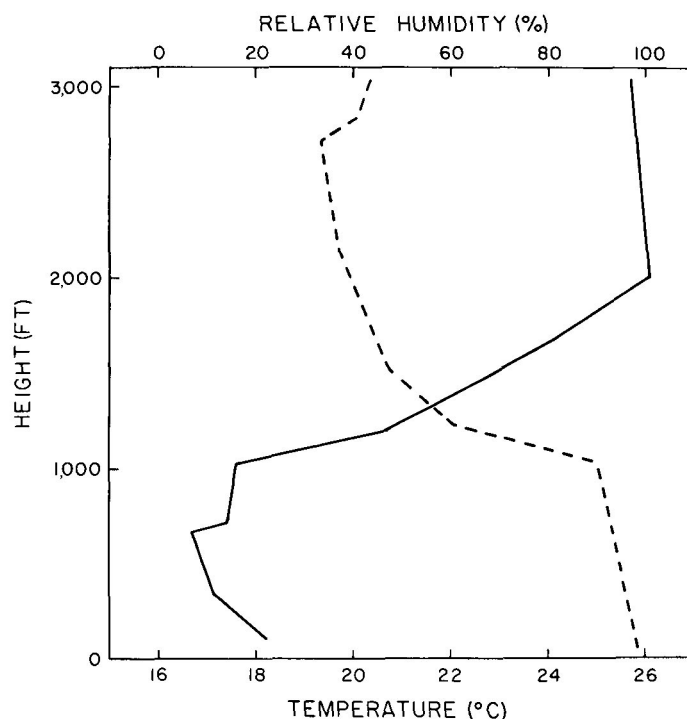


FIGURE 8.—Sounding associated with figure 7; profiles show temperature (solid curve) and relative humidity (dashed curve).

Another example of the same pattern is contained in the TIROS satellite photograph of figure 9. Here, one sees the phenomenon in the lee of three islands, San Nicolas, San Clemente, and Guadalupe and, thus, concludes that the marine layer was stably stratified on this day over a rather large area. In none of the cases is the wave strong enough to produce a second downdraft region.

A part of the lee-wave phenomenon familiar to observers in mountainous areas is the Föhnwall, or rapid downdraft just in the lee of a crest. This type of flow is not limited to large escarpments, and an example may be seen in figure 10. (The flow is from upper right to lower left.) The fingerlike formations in the descending, evaporating cloud are characteristic.

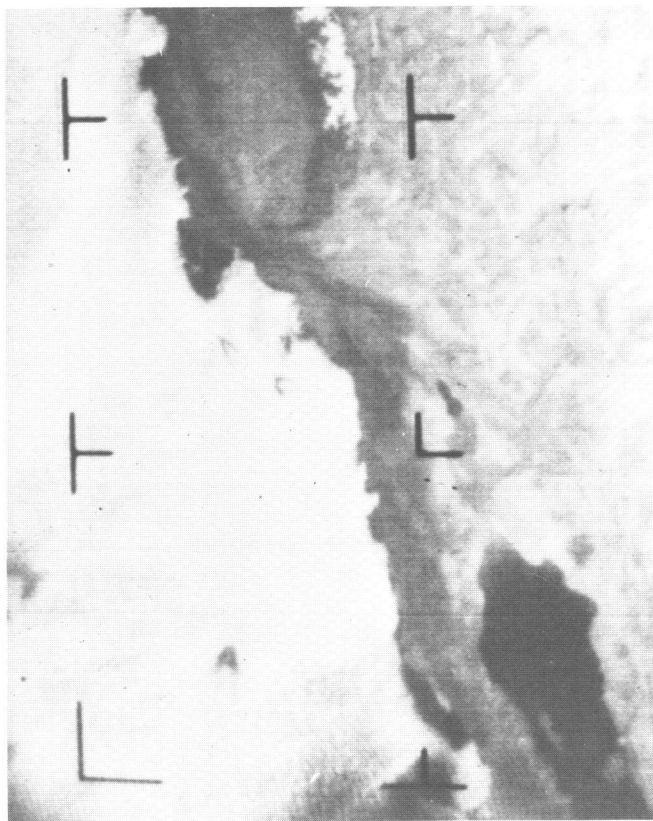


FIGURE 9.—June 20, 1967, TIROS satellite photograph. Baja California and the Gulf of California are in lower right corner, the Sierra Nevada, in upper center. Note breaks in stratus in the lee of San Nicolas, San Clemente, and Guadalupe Islands.

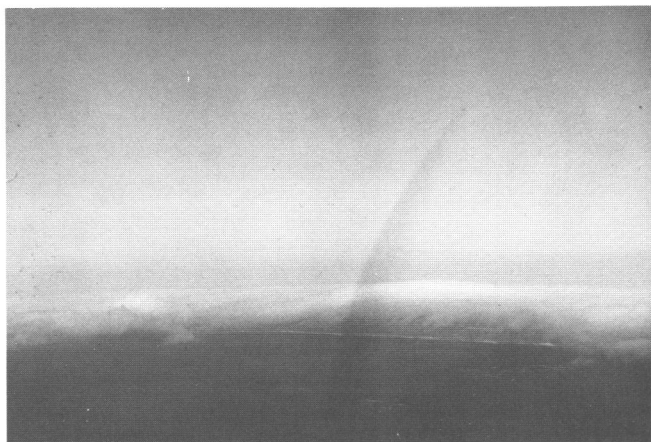


FIGURE 10.—Föhnwall in the lee of San Miguel Island. Flow is from upper right to lower left.

When the stability of the fluid is concentrated in an interface, flow over a limited obstacle will produce not the crescent-shaped pattern of the internal gravity waves, but rather something close to the classical Kelvin ship wave (sometimes called a bow wave—a nonexistent distinction in a theory that applies to a point source). Although this pattern is less frequently observed in the atmosphere, it is very familiar as a surface wave-system on water surfaces. Figure 11 contains a theoretical computation of the ship wave by Hogner (1922).

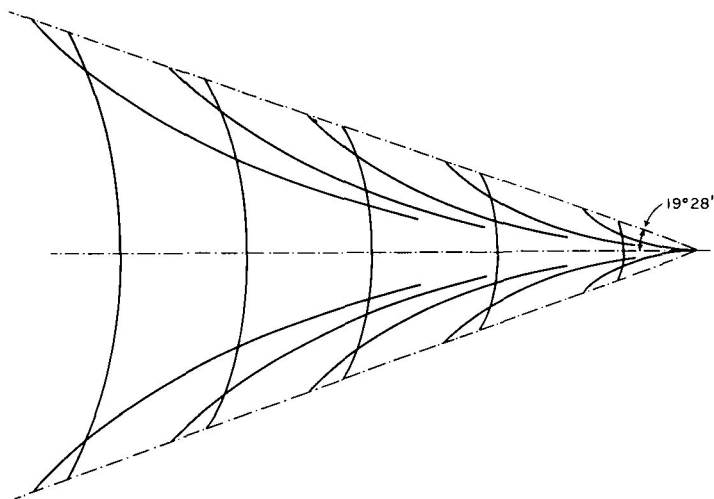


FIGURE 11.—Theoretical computation of the ship wave (Hogner 1922). The heavy lines mark the crests of the diverging and transverse wave systems. Flow is right to left.



FIGURE 12.—One branch of ship wave in the lee of San Nicolas Island. The flow is from lower right to upper left, and the island is just off the bottom of the photo.

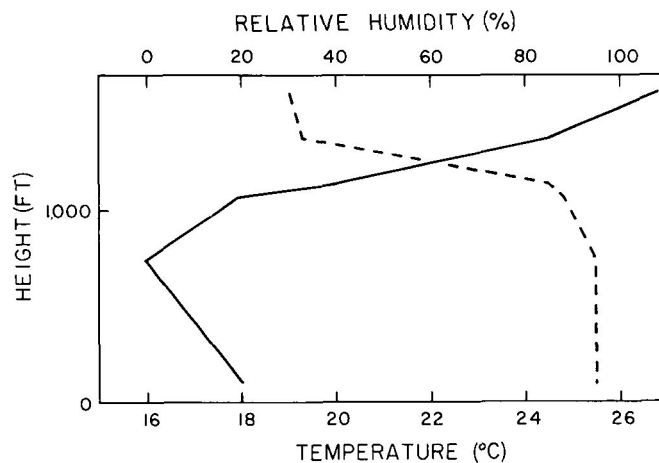


FIGURE 13.—Sounding associated with figure 12; profiles of temperature (solid curve) and relative humidity (dashed curve).

In addition to the Kelvin model, we have available computations by Scorer and Wilkinson (1956) for a two-layer atmosphere in which *both* layers are stably



FIGURE 14.—Area of descending motion over San Nicolas Island and adjacent ocean. Flow is left to right, and the island begins at the far left of the photograph.

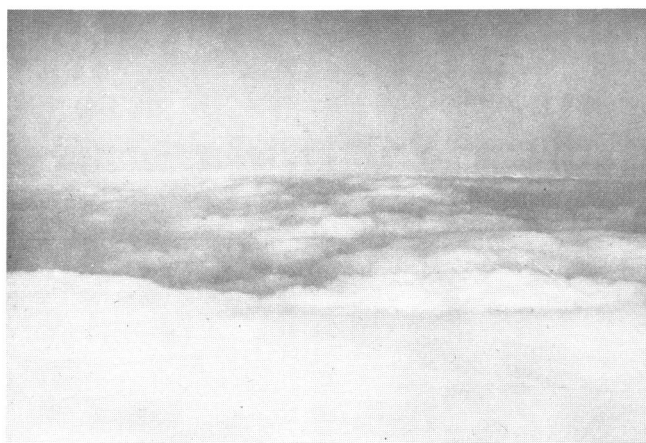


FIGURE 15.—Same as figure 14, but looking directly downwind. The stratus closing in just downwind of the island is evident.

stratified with a greater stability in the lower layer than in the upper. The only major difference in the patterns is that the half-angle containing the disturbance ($19^{\circ}28'$ in fig. 11) is reduced to about 12° in the two-layer atmospheric model. This difference exists because the discontinuity at the interface is assumed to be in the vertical gradient of density rather than in the density itself, as in the ship wave.

An illustration of the atmospheric ship wave in the lee of San Nicolas Island is shown in figure 12. It is not possible from our data to determine with sufficient accuracy the angle containing the disturbance. The sounding upwind of the island (fig. 13), however, shows that the clouds are observed at the top of an adiabatic layer, which would indicate that the hypothesis of the classical theory is more nearly fulfilled than that of Scorer and Wilkinson (1956). It will be noted that transverse wave-system is not evident in figure 12, but it is common in photographs of ship waves, even on water, to observe only the diverging wave-system.

A much more rare cloud pattern associated with flow over an island is shown in figures 14 and 15. Here the area of clear air was primarily over the land mass and extended sufficiently far over the water both cross wind

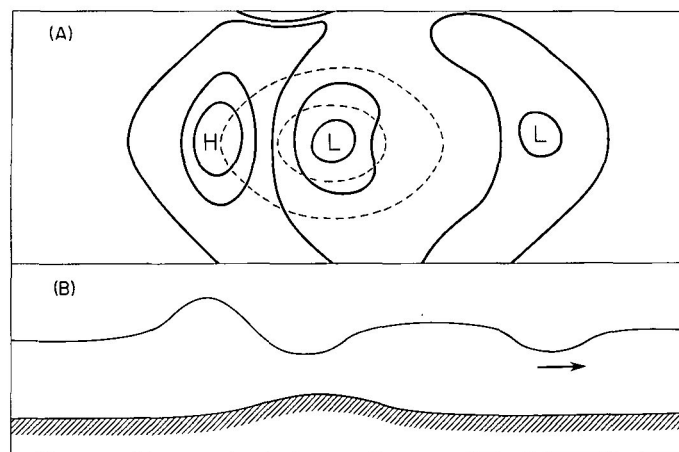


FIGURE 16.—(A) contours of free surface (solid lines) and bottom (dashed lines) in nonlinear shallow water flow. (B) profiles of free surface and bottom in a vertical section along the x-axis (after Wurtele and Lamb 1969).

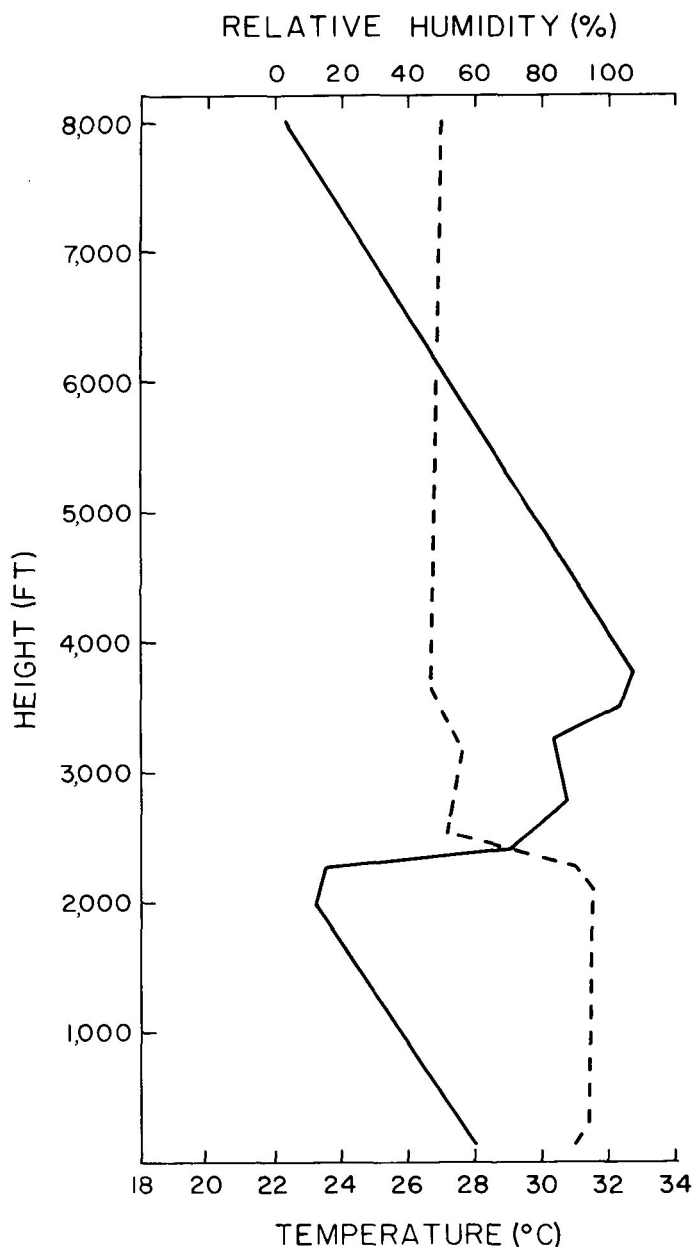


FIGURE 17.—Sounding associated with figures 14 and 15; profiles of temperature (solid curve) and relative humidity (dashed curve).



FIGURE 18.—Convective stratus over Santa Barbara Island.

and down wind, so that we deduce that descending motion rather than surface heating must be responsible for the break in the cloud deck. (The stratocumulus clouds over the island are probably the result of convective heating.) The best theoretical model for this pattern seems to be that of nonlinear shallow-water theory that would apply to two adiabatic layers with a potential temperature difference across the interface. If the Froude number and the ratio of the island height to the inversion height are sufficiently small, the one-dimensional theory (Houghton and Kasahara 1968) predicts a depression of the interface just over the obstacle. This simple result might be expected in two dimensions also, and computations with the nonlinear shallow-water equations (Wurtele and Lamb 1969) show this to be the case. Figure 16 show the contours of the interface for a Froude number of 0.3 and an island-to-inversion height ratio of 0.25. The inversion is lifted windward of the island and depressed just over it. (The depression further downstream is a transient phenomenon moving off to the right.) The height ratio in the observed instance is about 0.39; but the Froude number was 0.15, so that the same regime would be expected theoretically.

The sounding for this case is reproduced in figure 17. Note that the layers *both* below and above the interface are almost adiabatic. This unusual condition conforms to the hypotheses of the theory. So far as the sounding is concerned, a nonhydrostatic, or billow-cloud type of wave is also a possibility, and we cannot explain why the shallow-water mode seems so clearly to be preferred. (San Nicolas Island is about 10 mi long.)

For contrast, we present figure 18, in which the marine layer over the ocean is clear, but a convective stratus is formed just over Santa Barbara Island and over the very small island to the right.

4. OPTICAL BACK-SCATTER FROM THE STRATUS

The flights above the stratus deck presented frequent opportunities to observe and photograph glories. The glory—or anti-corona, in the terminology of van de Hulst (1947)—consists of light back-scattered from a

cloud of particles at angles close to 180° , the precise angle depending on the wavelength of the light. The observer sees one or more series of colored bands. The theory interpreting the glory as a Mie-scattering phenomenon rather than an example of geometric optics is due to van de Hulst (1947). However, the computations from the Mie theory are formidable in that a large number of scatterers are involved and a very large number of terms must be included. Thus, with the work of Deirmendjian (1969), it is possible to identify a cloud of a certain size distribution of drops with a corresponding scattering pattern. This is done as follows. Figures 19A–19D are drafted from data in the tables of Deirmendjian. The cloud types were selected by him as follows:

- C1—broad drop-size distribution with mean radius about $5\ \mu\text{m}$.
- C2—medium drop-size distribution with mean radius about $4\ \mu\text{m}$.
- C3—narrow drop-size distribution with mean radius about $2\ \mu\text{m}$.
- C4—narrow drop-size distribution with mean radius about $4\ \mu\text{m}$.

The wavelengths selected were in the blue ($0.45\ \mu\text{m}$) and red ($0.70\ \mu\text{m}$). It is evident that, in general, the larger the drops, the nearer to 180° is the peak in the scattering coefficient. In cloud type C4, the scatterers are large enough and homogeneous enough to produce double maxima in the back-scattering, and hence a double glory. We do not pretend, of course, that a given glory will determine uniquely a corresponding drop-size distribution, but only that our observations are consistent with the measured distribution types.

We have traced the glories of figure 20 from photographs with identical enlargements. The angle subtended by the various glory rings can be most accurately determined from the glory radius measured on the 35-mm transparency, knowing the focal length of the camera lens. Because the film is oriented normal to the sun's rays, the angle computed can be identified with the back-scatter angle.

Using figures 20A and 20B, we have measured the back-scattering angles given in table 1.

Thus, the cloud in figure 20B would seem to resemble the type C1 with perhaps an even larger mean radius and that of figure 20A to resemble the type C3 with a surprisingly small mean radius for stratus. Most of the glories observed fall between these two examples. We did not measure the drop-size distribution in the clouds, but earlier measurements (Neiburger and Wurtele 1949, p. 323) show the greatest frequency of droplet radii at about $7\ \mu\text{m}$ with a distribution near the cloud top much like that of Deirmendjian's type C4.

An example of multiple rings is that of figure 20C. This contains three sets of rings. We presume these to be associated with a cloud of very homogeneous drop distribution. For comparison purposes, we use Deirmendjian's data (1969, p. 54) for a single drop of radius $6.5\ \mu\text{m}$. The angles are given in table 2. We conclude that the cloud contained a large percentage of drops of just about this size.

On a number of occasions, the shadow of the airplane was quite visible on the cloud with no colored rings about it. Although we have no computations for clouds

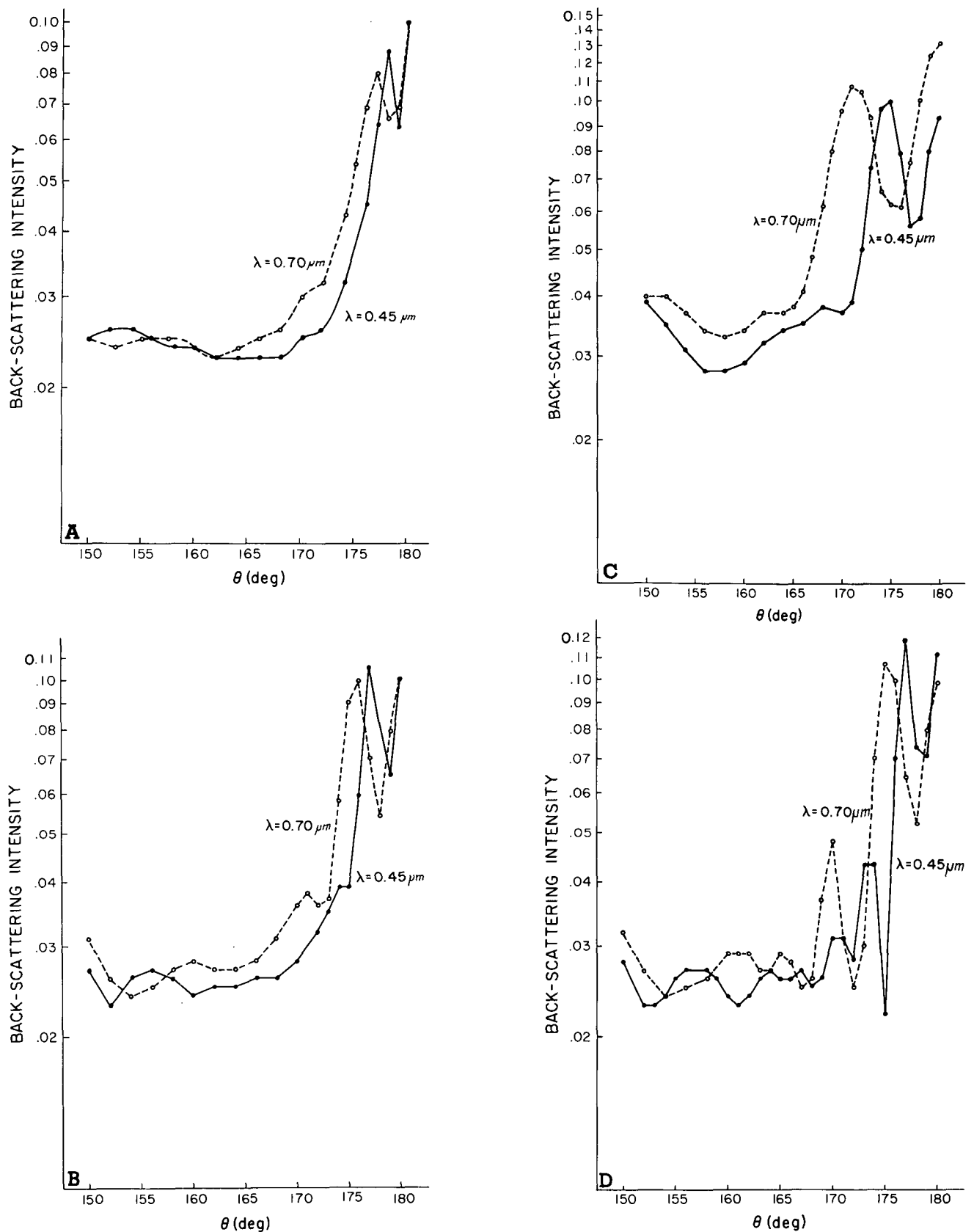


FIGURE 19.—Back-scattering intensity as a function of angle from data of Deirmendjian (1969). The solid line is for wavelength in the blue; dashed line in the red. The ordinate units are $P_1(\theta) + P_2(\theta)$ in the notation of the source. (A) cloud type C1; (B) cloud type C2; (C) cloud type C3; and (D) cloud type C4.

of broader distribution or larger mean radius than type C1, it is likely that such properties must have been responsible for this occasional absence of the glory.

Our present data suggest considerable variability, both within a given cloud and between different clouds. From the photographs of each run across a stratus

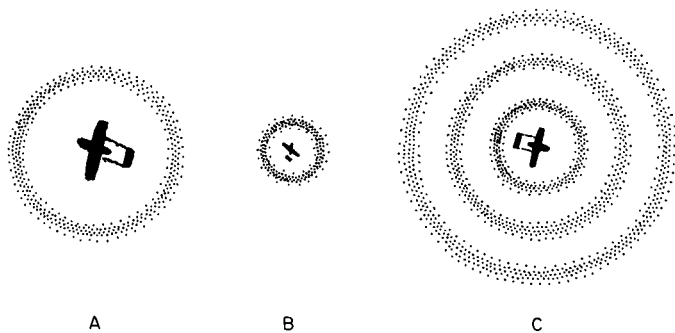


FIGURE 20.—Glory on stratus top with (A) large- and (B) small-diameter rings and (C) with multiple ring system.

TABLE 1.—Back-scattering angles (deg.) measured from figures 20A and 20B

| | Figure | |
|-----------------------------|--------|--------|
| | 20A | 20B |
| Red (outer) edge of ring | 171. 6 | 176. 6 |
| Yellow (inner) edge of ring | 173. 6 | 177. 1 |

TABLE 2.—Back-scattering angles (deg.) measured from figure 20C

| Glory ring | Observed | Deirmendjian |
|---------------|----------|--------------|
| 1st red ring: | 175. 9 | 176. 8 |
| 2d red ring: | 173. 2 | 173. 6 |
| 3d red ring: | 170. 1 | 170. 5 |

TABLE 3.—Observed frequency of occurrence of back-scatter angles of the first glory ring

| Back-scatter angle (deg.) | No. of observations |
|---------------------------|---------------------|
| 179. 0-178. 1 | 2 |
| 178. 0-177. 1 | 9 |
| 177. 0-176. 1 | 20 |
| 176. 0-175. 1 | 10 |
| 175. 0-174. 1 | 4 |
| 174. 0-173. 1 | 1 |
| 173. 0-172. 1 | 0 |
| 172. 0-171. 1 | 1 |

deck, we have taken the smallest, the modal, and the largest back-scattering angles of the first ring. The statistics from this survey are assembled in table 3.

Although these measurements would seem to indicate a somewhat smaller mean radius than that reported by Neiburger and Wurtele (1949), we consider that the agreement achieved by these two quite independent methods is satisfactory.

5. NOTE ON TERMINOLOGY

The term billow cloud is ambiguously used in the literature. The best-known treatment, perhaps, is that of

Haurwitz (1941, p. 287). He interprets a cloud as a wave on an interface across which an unstable velocity discontinuity and a stable density discontinuity exist. This dynamic model is easily extended to one containing an unstable velocity profile and a stable density profile, both with continuous variation (e.g., Ludlam 1967). The Haurwitz model is, of course, a limiting case of this. Both models are two dimensional, and the billows are oriented normal to the wind shear.

An unstable density (or potential temperature) gradient and a stable (e.g., linear) velocity profile, as shown by Eliassen et al. (1953) and Kuo (1963), can produce by convection a uniform alternating pattern of updrafts and downdrafts oriented along the wind direction. We have used the term longitudinal rolls for the convective phenomenon and reserved the term billow clouds for the shearing instability models. However, other authors (Ludlam and Scorer 1957, p. 72) expressly use billow to cover both dynamic phenomena.

ACKNOWLEDGMENTS

The field observations were made possible by the Pacific Missile Range, U.S. Navy, Point Mugu, Calif., under Contract No. N123 (61756)56992A. The theoretical work was done under grants NSF G-10167 and WBG-87.

In the field work, we were assisted in various ways by Dan Dibble, Gerald Chesebrough, Roger Helvey, and Arnold London, to whom we are most grateful.

The authors also wish to thank Douglas K. Lilly for valuable comments in his referee's report.

REFERENCES

- Angell, James K., and Pack, Donald H., "Helical Circulations in the Planetary Boundary Layer." *Physics of Fluids Supplement*, Vol. 10, No. 9, Pt. 2, Sept. 1967, pp. S226-S229.
- Avsec, Dusan, "Tourbillons thermoconvectifs dans l'air. Applications À La Météorologie" (Thermoconvective Eddies in Air—Applications to Meteorology), *Publications scientifiques et techniques* No. 155, Ministère de l'air, Paris, France, 1939, 214 pp.
- Brown, Robert A., "A Secondary Flow Model for the Planetary Boundary Layer," *Journal of the Atmospheric Sciences*, Vol. 27, No. 5, Aug. 1970, pp. 742-757.
- Deardorff, James Warner, "A Three-Dimensional Numerical Investigation of the Idealized Planetary Boundary Layer," *Geophysical Fluid Dynamics*, Vol. 1, No. 4, Gordon & Breach Science Publishers, London, England, Nov. 1970, pp. 377-410.
- Deirmendjian, Diran, *Electromagnetic Scattering on Spherical Polydispersions*, American Elsevier Publishing Co., Inc., New York, N.Y., 1969, 290 pp.
- Edinger, James G., and Wurtele, Morton G., "The Marine Layer Over Sea Test Range," *Final Report*, Contract No. N123(61756) 56992A, University of California, Los Angeles, 1969, 98 pp.
- Eliassen, Arnt, Hoiland, Einar, and Riis, Eyvind, "Two-Dimensional Perturbation of a Flow With Constant Shear of a Stratified Fluid," *Publication* No. 1, Institute of Theoretical Astrophysics, Oslo, Norway, 1953, 30 pp.
- Faller, Alan J., "Large Eddies in the Atmospheric Boundary Layer and Their Possible Role in the Formation of Cloud Rows," *Journal of the Atmospheric Sciences*, Vol. 22, No. 2, Mar. 1965, pp. 176-184.
- Greenspan, H. P., *The Theory of Rotating Fluids*, Cambridge University Press, England, 1968, 327 pp.
- Haurwitz, Bernhard, *Dynamic Meteorology*, McGraw-Hill Book Co., Inc., New York, N.Y., 1941, 365 pp.

- Hogner, Einar, "A Contribution to the Theory of Ship Waves," *Arkiv för Matematik, Astronomi och Fysik*, Vol. 17, No. 1, Svenska vetenskaps-akademien, Stockholm, Sweden, **1922**, pp. 1-50.
- Houghton, David D., and Kasahara, Akira, "Non-Linear Shallow Fluid Flow Over an Isolated Ridge," *Communications on Pure and Applied Mathematics*, Vol. 21, No. 1, Jan. **1968**, pp. 1-23.
- Kao, Shih-Kung, "Stationary Flow in the Planetary Boundary Layer With an Inversion Layer and a Sea Breeze," *Journal of Geophysical Research*, Vol. 65, No. 6, June **1960**, pp. 1731-1736.
- Kuo, Hsiao-Lan, "Perturbations of Plane Couette Flow in Stratified Fluids and Origin of Cloud Streets," *Physics of Fluids*, Vol. 6, No. 2, Feb. **1963**, pp. 195-211.
- Lilly, Douglas K., "On the Instability of the Ekman Boundary Layer," *Journal of the Atmospheric Sciences*, Vol. 23, No. 5, Sept. **1966**, pp. 481-494.
- Lilly, Douglas K., "Models of Cloud-Topped Mixed Layers Under a Strong Inversion," *Quarterly Journal of the Royal Meteorological Society*, Vol. 94, No. 401, London, England, July **1968**, pp. 292-309.
- Ludlam, Frank H., "Characteristics of Billow Clouds and Their Relation to Clear-Air Turbulence," *Quarterly Journal of the Royal Meteorological Society*, Vol. 93, No. 398, London, England, Oct. **1967**, pp. 419-435.
- Ludlam, Frank Henry, and Scorer, Robert S., *Cloud Study—A Pictorial Guide*, John Murray, London, England, **1957**, 80 pp.
- Malkus, Joanne Starr, and Riehl, Herbert, *Cloud Structure and Distributions Over the Tropical Pacific Ocean*, University of California Press, Berkeley, **1964**, 229 pp.
- Neiburger, Morris, "Temperature Changes During Formation and Dissipation of West Coast Stratus," *Journal of Meteorology*, Vol. 1, No. 1/2, Sept. **1944**, pp. 29-41.
- Neiburger, Morris, Johnson, David S., and Chien, Chen-Wu, "Studies of the Structure of the Atmosphere Over the Eastern Pacific Ocean in Summer, Pt. 1. The Inversion Over the Eastern North Pacific Ocean," *Publications in Meteorology*, Vol. 1, No. 1, University of California Press, Berkeley, **1961**, pp. 1-94.
- Neiburger, Morris, and Wurtele, Morton G., "On the Nature and Size of Particles in Haze, Fog, and Stratus of the Los Angeles Region," *Chemical Reviews*, Vol. 44, No. 2, Baltimore, Md., Apr. **1949**, pp. 321-335.
- Scorer, Robert S., "Airflow Over an Isolated Hill," *Quarterly Journal of the Royal Meteorological Society*, Vol. 82, No. 351, London, England, Jan. **1956**, pp. 75-81.
- Scorer, Robert S., and Wilkinson, Mary, "Waves in the Lee of an Isolated Hill," *Quarterly Journal of the Royal Meteorological Society*, Vol. 82, No. 354, London, England, Oct. **1956**, pp. 419-427.
- Tatro, P. R., and Mollo-Christensen, E. L., "Experiments on Ekman Layer Instability," *Journal of Fluid Mechanics*, Vol. 28, No. 3, May 26, **1967**, pp. 531-544.
- van de Hulst, Hendrick Christoffel, "A Theory of Anti-Corona," *Journal of the Optical Society of America*, Vol. 37, No. 1, American Institute of Physics, Inc., Rochester, N. Y., Jan. **1947**, pp. 16-22.
- Wurtele, Morton G., "The Three Dimensional Lee Wave," *Beiträge zur Physik der Atmosphäre*, Vol. 29, No. 4, Frankfurt a.M., Germany, **1957**, pp. 242-252.
- Wurtele, Morton G., and Lamb, Vivian Ruhlig, University of California, Los Angeles, **1969**, 12 pp. (unpublished manuscript).

[Received May 17, 1971; revised November 15, 1971]